Supporting Information for

Systematic Study of Various Functionalization Steps for Ultrasensitive Detection of SARS-CoV-2 with Direct Laser-Functionalized Au-LIG Electrochemical Sensors

Caroline Ji-Mei Brustoloni[1], Pouya Soltan Khamsi[1,2,3], Vinay Kammarchedu[1,2,3], and Aida Ebrahimi[1,2,3,4*]

[1] *Department of Electrical Engineering, The Pennsylvania State University, University Park, PA 16802, United States*

[2]*Center for Atomically Thin Multifunctional Coatings, The Pennsylvania State University, University Park, PA 16802, United States*

[3] *Department of Materials Science and Engineering, The Pennsylvania State University, University Park, PA 16802, United States*

[4]*Department of Biomedical Engineering, The Pennsylvania State University, University Park, PA 16802, United States*

*Corresponding author: sue66@psu.edu

Sensor	Sensing Surface Modification	Biofunctionalization Parameters	Ref.
Voltametric EC SARS-CoV-2 NP sensor	G/PBA/EDC/Sulfo-NHS	Crosslinker: 2 h humidity chamber Antibody: 3 h room ambient Antigen: 1-10 min diffusion-dominated incubation	1
SARS-CoV-2 S FET	Si/SiO_2/G/PBASE	Crosslinker: 1 h ambient Antibody: 4 h ambient Antigen: 1 min diffusion-dominated incubation	2
Voltametric EC SARS-CoV-2 NP sensor	GCE/GO-Au/EDC/Sulfo-NHS/Ag	Crosslinker: 2 h ambient Antibody: 4 °C overnight Antigen: N.D.	3
Voltametric EC SARS-CoV-2 RBD sensor	Si/SiO_2/G/PBASE	Crosslinker: 1 h ambient Antibody: 4 h 4°C Antigen: 30 min diffusion-dominated incubation at 4 °C	4
SARS-CoV-2 S FET	Au	Physisorption of capturing antibodies to gold sensing gate Antigen: 5 min diffusion-dominated incubation	5
Voltametric EC SARS-CoV-2 RBD sensor	Paper/GO/EDC/Sulfo-NHS	Crosslinker: 1 h ambient Antibody: 1 h ambient Antigen: 30 min diffusion-dominated incubation	6
Impedance EC SARS-CoV-2 RBD, S1, and N Antibody sensor	Au/rGO/EDC/Sulfo-NHS	Crosslinker: 4 h humidity chamber Antibody: 4 h humidity chamber Antigen: <1 min diffusion-dominated incubation	7
Impedance EC SARS-CoV-2 Sensor	G/PBA/EDC/Sulfo-NHS	Crosslinker: 2 h humidity chamber Antibody: 3 4°C Antigen: 15 min pipette-mixing every 5 minutes for 30 s	**This work**

Table S1. Comparison of surface modification and COVID-19 detection methods. EC = electrochemical, NP = nucleocapsid protein, G = graphene, PBA = 1-Pyrenebutyric acid, EDC = 1-ethyl-3-(3-dimethylaminopropyl)carbodiimide hydrochloride, Sulfo-NHS = N-Hydroxysulfosuccinimide sodium, FET= field effect transistor, PBASE = 1-Pyrenebutanoic Acid Succinimidyl Ester, GCE= glassy carbon electrode, GO-Au= Au electrodeposited on graphene oxide, RBD = receptor-binding domain, S1 = spike 1 protein , N = nucleocapsid, and rGO = reduced graphene oxide

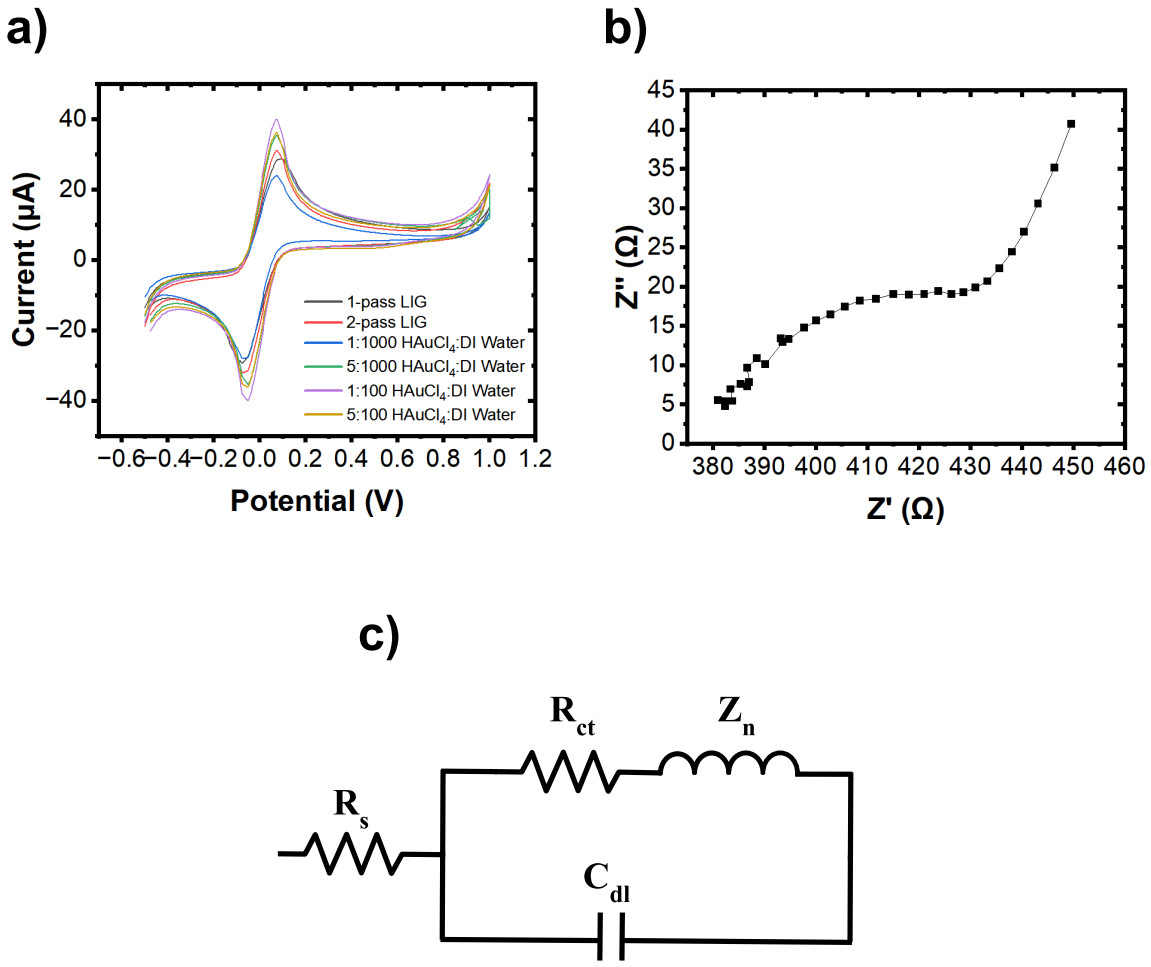

Figure S1. **Electrochemical sensor performance of 1-pass LIG, 2-pass LIG, and L-Au/LIG.** (a) Cyclic voltammetry (CV) curves with 1-pass LIG, 2-pass LIG, and L-Au/LIG functionalized with varying ratios of $HAuCl_4$: DI water. CV curves measured at a scan rate of 30 mV/s. Data are presented as mean (n=9). (b) A representative Nyquist plot measured using electrochemical impedance spectroscopy (EIS) for L-Au/LIG sensors after BSA treatment. (c) Randles equivalent circuit derived from EIS data where R_s is the solution resistance, R_{ct} is the charge-transfer resistance, C_{dl} is the double layer capacitance, and Z_n is the diffusional impedance (i.e. the Warburg impedance).

Incubation Environment	Γ (mol.mm^{-2})
PBASE (1 h, ambient), Antibody (12 h, RT)	$3.03 \pm 1.23 \times 10^{-10}$
PBASE (1 h, ambient), Antibody (3 h, RT)	$7.25 \pm 1.67 \times 10^{-10}$
PBASE (1 h, 97% humidity), Antibody (3 h, RT)	$8.82 \pm 0.96 \times 10^{-10}$
PBASE (1 h, 97% humidity), Antibody (3 h, 4°C)	$1.37 \pm 0.37 \times 10^{-9}$
PBASE (1.5 h, 97% humidity), Antibody (3 h, 4°C)	$1.08 \pm 0.13 \times 10^{-9}$
PBASE (3 h, 97% humidity), Antibody (3 h, 4°C)	$8.96 \pm 2.86 \times 10^{-10}$
PBA (35 min, 97% humidity), Sulfo-NHS: EDC (1 h, humidity), Antibody (3 h, 4°C)	$1.04 \pm 0.21 \times 10^{-9}$
PBA (35 min, 97% humidity), Sulfo-NHS: EDC (2 h, humidity), Antibody (3 h, 4°C)	$1.86 \pm 0.22 \times 10^{-9}$
PBA (35 min, 97% humidity), Sulfo-NHS: EDC (3 h, humidity), Antibody (3 h, 4°C)	$7.68 \pm 0.89 \times 10^{-10}$

Table S2. Studying the effect of the incubation environment during the crosslinker and antibody treatment. Γ is surface coverage density of antibodies. Data is presented as mean (n=9), and error is standard deviation.

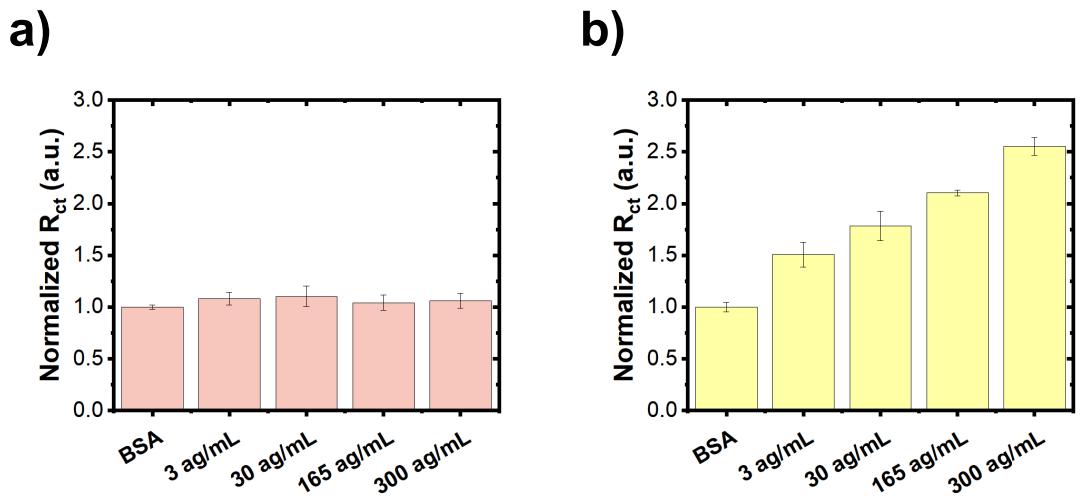

Figure S2. **Studying the effect of diffusion-dominated incubation vs. pipette-mixing in E-Au/LIG sensors.** Normalized charge-transfer resistance of E-Au/LIG sensor (w.r.t. that of samples after BSA treatment) after incubation with various concentrations of SARS-CoV-2 antigen in PBS (a) using diffusion-dominated incubation method (data are presented as mean (n=12). Error bars are standard error of the mean [S.E.M.]), and (b) using pipette-mixing method (data are presented as mean (n=12). Error bars are S.E.M.). The studies are performed using PBA crosslinker chemistry.

Sensor	R^2	S $\left(\frac{\%}{\log(ag.mL^{-1})}\right)$	σ of Blank	LOD (ag. mL^{-1})
L-Au/LIG, PBASE, diffusion-dominated incubation	0.86	26	0.63	8.19
L-Au/LIG, PBA/Sulfo-NHS: EDC, diffusion-dominated incubation	0.88	35	0.71	6.69
1-pass LIG, diffusion-dominated incubation	0.95	47	0.54	3.75
1-pass LIG, pipette-mixing	0.85	33	0.43	4.25
2-pass LIG, pipette-mixing	0.99	30	0.054	0.59
L-Au/LIG, pipette-mixing	0.99	56	0.20	1.21
Artificial Saliva, L-Au/LIG, pipette-mixing	0.94	38	0.42	3.19

Table S3. Correlation coefficient, sensitivity, standard deviation (STD), and limit of detection (LOD) using calibration of sensors in response to antigen in buffer or artificial saliva. The calculated correlation coefficient (R^2), sensitivity (*S*) which is calculated by normalizing R_{ct} values w.r.t. R_{ct} of samples after BSA treatment, STD (σ) of blank sensor before exposure to antigen, and LOD from calibration curves (charge-transfer resistance vs. analyte concentration).

Limit of detection (LOD) and sensitivity (*S*) are some of the most important measures for benchmarking performance of biosensors. To evaluate LOD, the sensitivity and noise level of a blank sensor before exposure to antigen are calculated. The measurement sensitivity, defined as the relative change in R_{ct} normalized to a blank sensor (i.e. the sensor after BSA treatment) to decade change in antigen concentration, is calculated by linear fitting of the calibration curves in Fig. 5 and Fig. 6. The noise level is calculated with the standard deviation (STD, σ) of 3 repeated measurements each of 3 blank sensors. The limit of detection is defined as 3.3σ/S.[8] Table S2 lists the calculated correlation coefficient (R^2 to signal the linearity of fitting), sensitivity, STD of blank sensor, and LOD from the calibration curves of sensors fabricated with varying fabrication parameters detailed in the following sections.

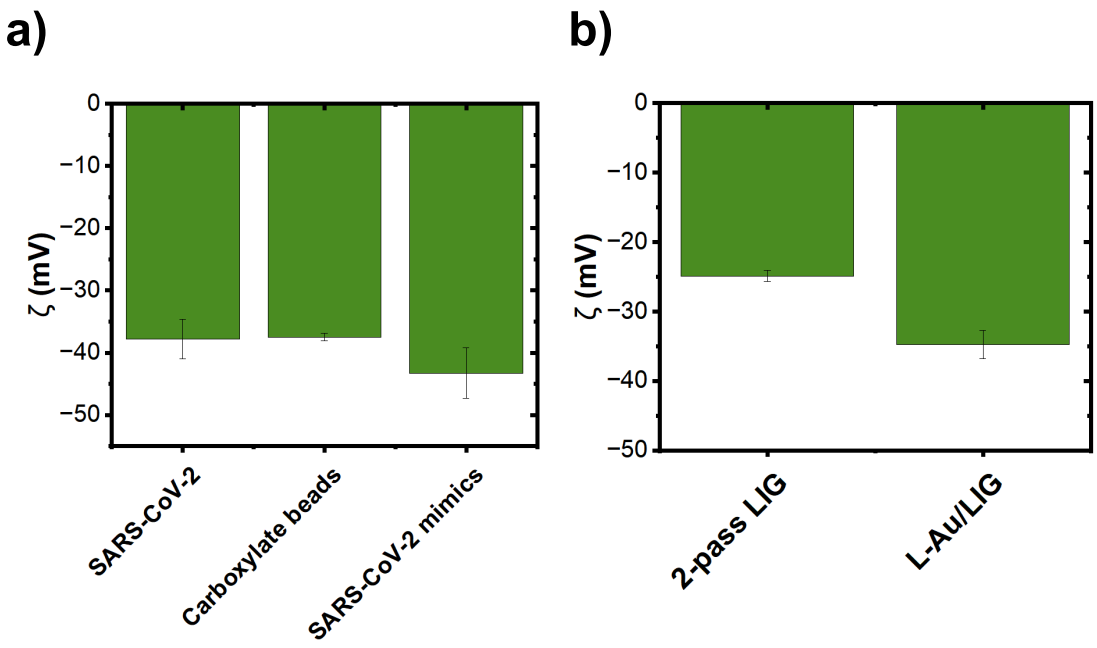

Figure S3. Zeta potential measurements of SARS-CoV-2 antigen, 2-pass LIG, and L-Au/LIG. (a) Zeta potential measurements of SARS-CoV-2 (heat-inactivated), carboxylate beads (100 nm), and SARS-CoV-2 mimics (made using 100 nm carboxylate beads) adapted from a previous study.[9] Data are presented as mean (n=3). Error bars are standard deviation (STD). (b) Zeta potential measurements of 1-pass LIG and L-Au/LIG sensor surface. Data are presented as mean (n=3). Error bars are STD.

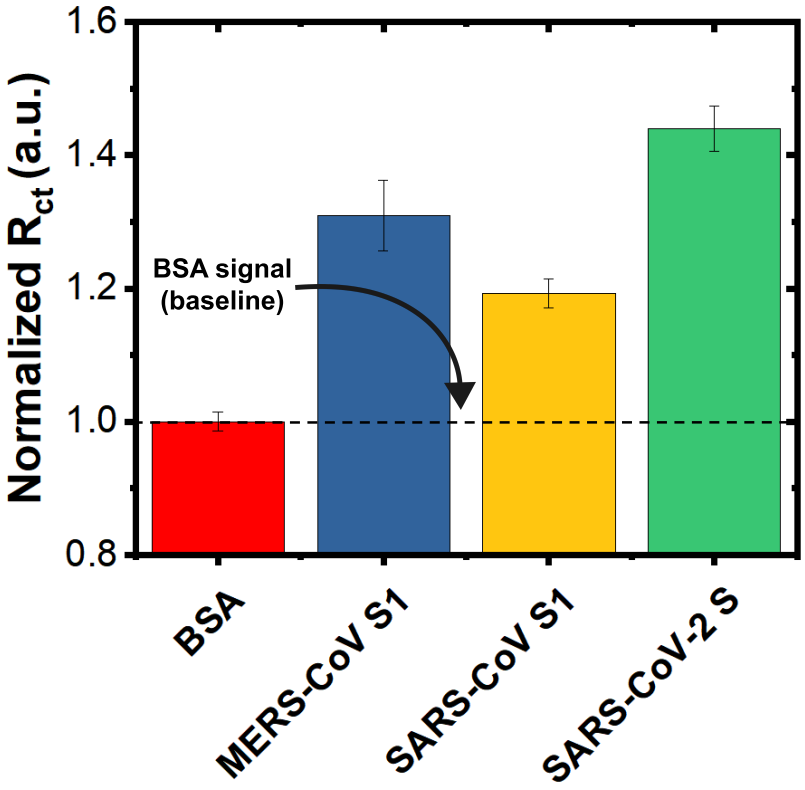

Figure S4. **Cross reactivity of the sensors with MERS and SARS-CoV S1.** SARS-CoV-2 antigen and interferential molecules were tested at 30 ag.mL^{-1}in PBS. Data are presented as mean (n=9). Error bars are standard error of the mean.

Sensor	R^2	$\left(\frac{S}{\log(particles.mL^{-1})}\right)$	σ of Blank	LOD $(particles.mL^{-1})$
Virus Mimic 2-pass LIG	0.95	27	0.050	~5
Virus Mimic L-Au/LIG	0.26	n.d.	0.027	n.d.

Table S4. Correlation coefficient, sensitivity, standard deviation (STD), and limit of detection (LOD) using calibration in response to virus mimics. The calculated correlation coefficient (R^2), sensitivity (S) which is calculated by normalizing R_{ct} values w.r.t. R_{ct} of samples after BSA treatment, STD (σ) of blank sensor before exposure to antigen, and LOD from calibration curves.

Sensor	LOD	S and Linear Range	Sample, Selectivity	Sensor-Readout	Ref.
Voltametric EC sensor for SARS-CoV-2 NP antigen	500 pg.mL^{-1}	S = ~-0.8 $\frac{nA}{\text{pg}.mL^{-1}}$ from 500 pg.mL^{-1} to 5000 pg.mL^{-1}	Fragment antigen in PBS and human serum, clinical samples (qualitative +/- detection) Selectivity tested against SARS-CoV-2 S1, SARS-CoV S1, SARS-CoV NP (cross reaction)	Wireless PCB-based platform	1
FET sensor for SARS-CoV-2 S antigen	1 fg.mL^{-1} (PBS) 100 fg.mL^{-1} (UTM) 1.6 x 10^1 pfu.mL^{-1} (culture medium in UTM) 2.42 x 10^2 copies.mL^{-1}(clinical samples in UTM)	S =~0.2 $\frac{a.u.}{\log(\text{fg}.mL^{-1})}$ (PBS) from ~10 fg.mL^{-1} to ~10^3 fg.mL^{-1} (PBS) S = ~0.008 $\frac{a.u.}{\log(\text{pg}.mL^{-1})}$ (UTM) from ~10^{-1} pg.mL^{-1} to ~10^2 pg.mL^{-1} (UTM) S = ~0.005 $\frac{a.u.}{\log(\text{pfu}.mL^{-1})}$ (cultural samples in UTM) from 1.6 x 10^1 pfu.mL^{-1} to 1.6 x 10^4 pfu.mL^{-1} (cultural samples in UTM) S = ~0.004 $\frac{a.u.}{\log(\text{copies}.mL^{-1})}$ (clinical sample in UTM) from ~10^{-1} pg.mL^{-1} to ~10^2 pg.mL^{-1} (clinical sample in UTM)	Fragment antigen in PBS and UTM, culture medium in UTM, clinical samples in UTM (qualitative) Selectivity tested against MERS-CoV	2634B Keithly semiconductor analyzer and probe station	2

Voltametric EC sensor for SARS-CoV-2 NP antigen	3.99 ag. mL^{-1} in PBS	$S = 2.33\frac{\mu A}{\log(\text{fg}.mL^{-1})}$ from 10.0 ag. mL^{-1} to 75.0 pg. mL^{-1}	Fragment antigen in PBS, patient samples (qualitative detection) Selectivity tested against immunoglobin M, immunoglobin G, glutathione, and L-tryptophan	Autolab potentiostat	3
Voltametric EC sensor for SARS-CoV-2 RBD antigen	1 fg. mL^{-1} (PBS) 3.75 fg. mL^{-1} (artificial saliva)	$S = \sim\text{-}17\ \frac{meV}{log(\text{pg}.mL^{-1})}$ from 0.5 to 4 fg. mL^{-1}	Fragment antigen in PBS and artificial saliva Selectivity tested against MERS-CoV	Raman-AFM WITec alpha 300 RA	4
SARS-CoV-2 S Antigen FET	Single marker/0.1 mL	N.D.	Patient saliva, blood, and nasal swab Selectivity tested against MERS-CoV	Wireless PCB-based platform	5
Voltametric EC sensor for SARS-CoV-2 RBD	0.11 ng. mL^{-1} in PBS	$S = \sim 7\ \frac{\mu A}{log(\text{pg}.mL^{-1})}$ From 1 ng. mL^{-1} to 1000 ng. mL^{-1}	Fragment antigen in PBS Selectivity tested against Hepatitis B surface antigen, Hepatitis-C virus	Emstat3 Blue wireless potentiostat	6
Impedance EC SARS-CoV-2 Sensor	1.21 ag. mL^{-1} (fragment) 5 particles/mL (virus mimic)	$S = 56\ \frac{\%}{\log(\text{ag}.mL^{-1})}$ (fragment) from 3 ag. mL^{-1} to 300 ag. mL^{-1} $S = 27\ \frac{\%}{\log(\text{particles}.mL^{-1})}$ (virus mimic) from 200 to 20000 particles. mL^{-1}	Fragment antigen and antigen-coated virion mimics in PBS and artificial saliva, patient samples (qualitative) Tested against HCoV-229E, HCoV-OC43, HCoV-NL63, H5N1, MERS-CoV (cross reaction), and SARS-CoV S1 (cross reaction)	Multipalmsens	**This work**

Table S5. Comparison of limit of detection (LOD), sensitivity (*S*), and selectivity of electroanalytical sensors for SARS-CoV-2. EC = electrochemical, NP = nucleocapsid protein, S1 = spike 1 protein, PCB = printed circuit board, S = spike, UTM = universal transport medium, PBS = phosphate buffered saline, RBD = receptor-binding domain, and FET = field effect transistor.

References

(1) Torrente-Rodríguez, R. M.; Lukas, H.; Tu, J.; Xu, C.; Rossiter, H. B.; Gao, W. SARS-CoV-2 RapidPlex: A Graphene-Based Multiplexed Telemedicine Platform for Rapid and Low-Cost COVID-19 Diagnosis and Monitoring. *Matter* **2020**, *3* (6), 1981–1998. https://doi.org/10.1016/j.matt.2020.09.027.

(2) Seo, G.; Lee, M. J.; Kim, S.-H.; Choi, M.; Ku, K. B.; Lee, C.-S.; Jun, S.; Park, D.; Kim, H. G.; Kim, S.-J.; Lee, J.-O.; Kim, B. T.; Chang, E.; Park, K.; Kim, S. I. Rapid Detection of COVID-19 Causative Virus (SARS-CoV-2) in Human Nasopharyngeal Swab Specimens Using Field-Effect Transistor-Based Biosensor. *ACS Nano* **2020**, *14* (4), 5135–5142. https://doi.org/10.1021/acsnano.0c02823.

(3) Sadique, M. A.; Yadav, S.; Ranjan, P.; Khan, R.; Khan, F.; Kumar, A.; Biswas, D. Highly Sensitive Electrochemical Immunosensor Platforms for Dual Detection of SARS-CoV-2 Antigen and Antibody Based on Gold Nanoparticle Functionalized Graphene Oxide Nanocomposites. *ACS Appl. Bio Mater.* **2022**, *5* (5), 2421–2430. https://doi.org/10.1021/acsabm.2c00301.

(4) Nguyen, N. H. L.; Kim, S.; Lindemann, G.; Berry, V. COVID-19 Spike Protein Induced Phononic Modification in Antibody-Coupled Graphene for Viral Detection Application. *ACS Nano* **2021**, *15* (7), 11743–11752. https://doi.org/10.1021/acsnano.1c02549.

(5) Macchia, E.; Kovács-Vajna, Z. M.; Loconsole, D.; Sarcina, L.; Redolfi, M.; Chironna, M.; Torricelli, F.; Torsi, L. A Handheld Intelligent Single-Molecule Binary Bioelectronic System for Fast and Reliable Immunometric Point-of-Care Testing. *Sci. Adv.* **2022**, *8* (27). https://doi.org/10.1126/sciadv.abo0881.

(6) Yakoh, A.; Pimpitak, U.; Rengpipat, S.; Hirankarn, N.; Chailapakul, O.; Chaiyo, S. Paper-Based Electrochemical Biosensor for Diagnosing COVID-19: Detection of SARS-CoV-2 Antibodies and Antigen. *Biosens. Bioelectron.* **2021**, *176*, 112912. https://doi.org/10.1016/j.bios.2020.112912.

(7) Ali, M. A.; Zhang, G. F.; Hu, C.; Yuan, B.; Jahan, S.; Kitsios, G. D.; Morris, A.; Gao, S.; Panat, R. Ultrarapid and Ultrasensitive Detection of SARS-CoV-2 Antibodies in COVID-19 Patients via a 3D-Printed Nanomaterial-Based Biosensing Platform. *J. Med. Virol.* **2022**, *94* (12), 5808–5826. https://doi.org/10.1002/jmv.28075.

(8) Armbruster, D. A.; Pry, T. Limit of Blank, Limit of Detection and Limit of Quantitation. *Clin. Biochem. Rev.* **2018**, *29 Suppl 1* (Suppl 1), S49–S52. Available: https://www.ncbi.nlm.nih.gov/pmc/articles/PMC2556583/

(9) Khamsi, P. S.; Kammarchedu, V.; Ebrahimi, A. Evaporation-Enhanced Redox Cycling for Rapid Detection of Attomolar SARS-CoV-2 Virions Using Nanolithography-Free Electrochemical Devices. https://doi.org/10.1149/osf.io/j5qxk [under review].